AD-A048 618 RCA LABS PRINCETON N J F/G 11/6
BASIC ADHESION MECHANISMS IN THICK AND THIN FILMS.(U)
NOV 77 T T HITCH, K R BUBE N00019-77-C-0176
UNCLASSIFIED PRRL-77-CR-47 NL

1 OF 1
AD A048618

END
DATE FILMED
2-78
DDC

AD A048618

DDC
RECEIVED
JAN 12 1978
B

UNCLASSIFIED

SECURITY CLASSIFICATION OF THIS PAGE (When Data Entered)

REPORT DOCUMENTATION PAGE	READ INSTRUCTIONS BEFORE COMPLETING FORM
1. REPORT NUMBER (9) Quarterly rept. no. 3	2. GOVT ACCESSION NO. 3. RECIPIENT'S CATALOG NUMBER
4. TITLE (and Subtitle) (6) BASIC ADHESION MECHANISMS IN THICK AND THIN FILMS.	5. TYPE OF REPORT & PERIOD COVERED: Quarterly #3 (7-1-77 to 9-30-77)
	6. PERFORMING ORG. REPORT NUMBER: (14) PRRL-77-CR-47
7. AUTHOR(s) (10) Thomas T. Hitch [redacted] Kenneth R. Bube	8. CONTRACT OR GRANT NUMBER(s): (15) N00019-77-C-0176
9. PERFORMING ORGANIZATION NAME AND ADDRESS: RCA Laboratories, Princeton, New Jersey 08540	10. PROGRAM ELEMENT, PROJECT, TASK AREA & WORK UNIT NUMBERS
11. CONTROLLING OFFICE NAME AND ADDRESS: Naval Air Systems Command, Washington, DC 20361	12. REPORT DATE: (11) Nov [redacted] 77
	13. NUMBER OF PAGES: (12) 34p.
14. MONITORING AGENCY NAME & ADDRESS (if different from Controlling Office)	15. SECURITY CLASS. (of this report): Unclassified
	15a. DECLASSIFICATION/DOWNGRADING SCHEDULE: N/A

16. DISTRIBUTION STATEMENT (of this Report)

APPROVED FOR PUBLIC RELEASE: DISTRIBUTION UNLIMITED

DDC RECEIVED JAN 12 1978 B

17. DISTRIBUTION STATEMENT (of the abstract entered in Block 20, if different from Report)

18. SUPPLEMENTARY NOTES

19. KEY WORDS (Continue on reverse side if necessary and identify by block number)

Sintering Theory
Gold Powder
Liquid Phase Sintering
Reactive Bonding
Adhesion

20. ABSTRACT (Continue on reverse side if necessary and identify by block number)

This is the third quarterly report on the fourth in a series of ~~one-year~~ contracts at RCA to study adhesion mechanisms in thick-film conductors. In the study of frit-bonded materials this quarter, the sintering of gold powders was studied and indicated to be assisted by the presence of a lead borosilicate glass in the second stage of sintering (solution-precipitation) at higher temperatures. ~~Last~~

over

DD FORM 1 JAN 73 1473

UNCLASSIFIED

SECURITY CLASSIFICATION OF THIS PAGE (When Data Entered)

299 000

20.

quarter the glass had been shown to assist first-stage sintering (rearrangement).

The evolution of organic-vehicle-burnoff gas products from sintering gold and gold/glass powders was also investigated. For the materials studied, which were typical of thick-film paste constituents, it was concluded that organic burnout should not interfere with the sintering of most gold powders. It was further determined that at the completion of burnout, the organic burnoff gases should be able to escape through the glass phase rapidly enough to prevent their entrapment in the partially sintered structure.

In the reactively bonded conductor phase of the work a study was made of the effect of layering a gold ink containing no binder onto the top of a binder layer of CuO, CdO, or mixture of CuO and CdO which had been prefired over a range of temperatures and etched. When the overlay gold films were fired at the lower temperature (900°C), they were more adherent to the CdO and 3CdO:1CuO (by wt) layers fired at higher temperatures. When the overlay firing temperature was increased, the adhesion was greater to the CuO and 3CuO:1CdO binder layers that had been fired at the higher temperature.

In related experiments on the reactive bonding mechanism, the weight gains of substrates reacted with films of CdO, CuO, and mixtures of the oxides were studied as a function of temperature. The thermal activation data found differs from that of Lisauskas (for CdO and CuO, which was discussed last quarter). The highest weight gains and largest activation energies were those for the mixed CdO and CuO films.

APPROVED FOR PUBLIC RELEASE
DISTRIBUTION UNLIMITED

PREFACE

This quarterly report describes work performed in the Integrated Circuit Technology Center of RCA Laboratories, under Contract No. N00019-77-C-0176 and under RCA funds. Mr. J. H. Scott, Jr., is the Laboratory Director and Dr. G. L. Schnable, the Project Supervisor and Group Head. Dr. Thomas T. Hitch is the Project Scientist and with Mr. K. R. Bube comprises the principal research team. Mr. James Willis is the Government Project Monitor.

It is a pleasure to acknowledge the help of a number of individuals who are contributing to this study by the performance of several analytical techniques. Notable are Mr. R. J. Paff for the x-ray diffraction and Mr. B. J. Seabury for scanning electron microscopy. We particularly acknowledge the able assistance of Mr. E. J. Conlon and Mr. A. Z. Miller in the preparation of samples for analysis and in the day-to-day pursuit of the study. Discussions throughout the study with Dr. G. L. Schnable and his reviews of the manuscript have been most valuable.

Space does not permit mentioning all the persons who have contributed to this study, but we acknowledge helpful discussions with the scientists studying thick-film technology at Purdue University and the Naval Research Laboratories; the Project Monitor, Mr. James Willis; and his supervisor, Dr. Herbert J. Mueller.

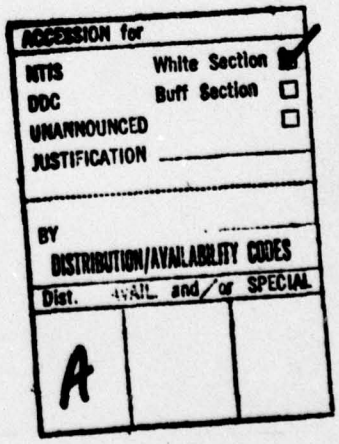

TABLE OF CONTENTS

Section		Page
I.	INTRODUCTION	1
II.	FRIT-BONDED CONDUCTORS	2
	A. Organic Binder Combustion Test	2
	B. MK-2 Au Densification in the Presence of E1527 Glass	3
	C. Activation Energies for the Sintering of Gold in the Presence and Absence of Glass	9
III.	REACTIVELY BONDED CONDUCTORS	18
	A. Interface Compound Formation Studies	18
	1. Procedure	18
	2. Results	19
	B. Binder Layer/Overlay Experiments	24
	C. Discussion	24
IV.	FUTURE WORK	26
REFERENCES		27

LIST OF ILLUSTRATIONS

Figure		Page
1.	Polymer combustion rate	3
2.	Normalized densification at 30 s vs temperature and glass content	6
3.	Normalized densification at 600 s vs temperature and glass content	6
4.	Normalized densification at 10 vol pct glass vs temperature and time	8
5.	Diametral change vs $t^{0.31}$ at 700°, 800°, and 900°C for glass-free MK-2 Au	9
6.	Diametral change vs $t^{0.31}$ at 700°, 800°, and 900°C for MK-2 Au with 10 vol pct E1527 glass	10
7.	The reaction of CuO films with 96 wt pct alumina substrates as a function of temperature	20
8.	The reaction of 3CuO:1CdO weight mixture films with 96 wt pct alumina substrates as a function of temperature	20
9.	The reaction of 3CdO:1CuO weight mixture films with 96 wt pct alumina substrates as a function of temperature	21
10.	The reaction of CdO films with 96 wt pct alumina substrates as a function of temperature	21

LIST OF TABLES

Table		Page
1.	Density of E1527 Glass vs Firing Time at 900°C	4
2.	Percent Weight Loss of Powder Compacts	7
3.	Diametral and Density Changes of MK-2 Au	11
4.	Diametral and Density Changes of MK-2 Au with 10 Volume Percent E1527 Glass	12
5.	Summary of Activation Energies	15
6.	Summary of Sintering Kinetics of Powder Compacts	17
7.	The Character and Appearance of Thermally Reacted Oxide Films on Coors ADS 96F Substrates	22
8.	Thermal Activation Coefficients for Weight Changes Due to Oxide Film Reactions with 96 Wt Pct Alumina Substrates	23
9.	Results of Scotch-Tape Adhesion Strength Test on Overlay Gold Films Fired Onto Thermally Reacted Oxide Layers on Coors ADS96F Substrates	25

SECTION I

INTRODUCTION

The work presented here was performed or completed in the third quarter of Naval Air Systems Command Contract No. N00019-77-C-0176. The contract is devoted to improvement in the understanding of thick-film conductor materials through the study of the fundamental mechanisms of their adhesion. This contract is the fourth in a series. In the earlier contracts, commercial and model inks based on gold, on silver and copper, and on gold-platinum-(palladium) alloys were studied in successive years. This year's work is dependent on the findings of the earlier contracts.

The work presented in this report is divided into two sections. The first deals with frit-bonded conductors; the second, with mixed-bonded and reactively bonded conductors.

In earlier years it has been shown that for optimized adhesion strength frit-bonded conductors, particularly gold-based, frit-bonded conductors, depend more on physical (microstructural) conformation than do reactively bonded and mixed-bonded conductors. Accordingly, the frit-bonded work presented here includes the important areas of sintering with and without the presence of glass and of metal-to-frit interface disruption. Such disruptions are sometimes caused by the outgassing of gold powders in the latter stages of sintering when thick films are fired at higher temperatures.

That part of the report which concerns reactive and mixed bonding deals principally with the formation of chemical species at the interfaces that separate the metal and ceramic layers and with the identification of their role in adhesion.

SECTION II

FRIT-BONDED CONDUCTORS

A. ORGANIC BINDER COMBUSTION TEST

In all thick-film ink systems, the metal powder and glass frit are suspended in an organic vehicle. To enhance durability in the dried but unfired state, the inks contain organic polymer or resin which remains in the dried deposit prior to high-temperature firing. With a view to examining sintering kinetics and the interreactions of frit and metal, as well as achieving a dense deposit, the organic polymer should be thoroughly burned before significant sintering occurs. A typical polymeric additive is ethylcellulose dispersed in an appropriate solvent.

To assess the burnout rate of the polymer a quantity of high-molecular-weight, N-300 grade* ethylcellulose was dissolved in a mixture of Carbitol** [2-(2-ethoxyethoxy)ethanol] and butyl Carbitol [2-(2-butoxyethoxy)ethanol] to yield 10 wt pct polymer in a solution containing 25 wt pct Carbitol and 75 wt pct butyl Carbitol. For tares, polished alumina substrates measuring 1 in. x 1 in. x 0.005 in. were used. Onto the tares, the solution was doctor-bladed into a 0.75-in.-diameter hole in a 0.064-in.-thick Teflon (polytetrafluoroethylene) stencil†. After drying at 125°C for 45 min, the dried polymer film weighing 0.040 - 0.045 g was exposed to 300°, 400°, and 500°C respectively, in air flowing at 10 ft^3/h. The percent-weight-loss curves for these temperatures are plotted as a function of time in seconds in Fig. 1. From Fig. 1, it can be seen that only 3 s at 500°C or 17 s at 400°C suffices to burn the polymer completely. At 300°C the weight loss is still incomplete after 2 min. However, with reference to the sintering of fine particle size Au, for example MK-2 for 17 s at 400°C shows only a small percentage of total densification (Fig. 6, Quarterly Report No 2 [1]). The 0.040-g polymer test print covered a 0.75-in.

*Hercules Corp., Wilmington, DE.
**Union Carbide Corp., New York, NY.
†E. I DuPont de Nemours & Co., Inc., Wilmington, DE.

1. K.R. Bube and T.T. Hitch, "Basic Adhesion Mechanisms in Thick and Thin Films," Quarterly Report No. 2, NASC Contract No. N00019-77-C-0176, July 1977.

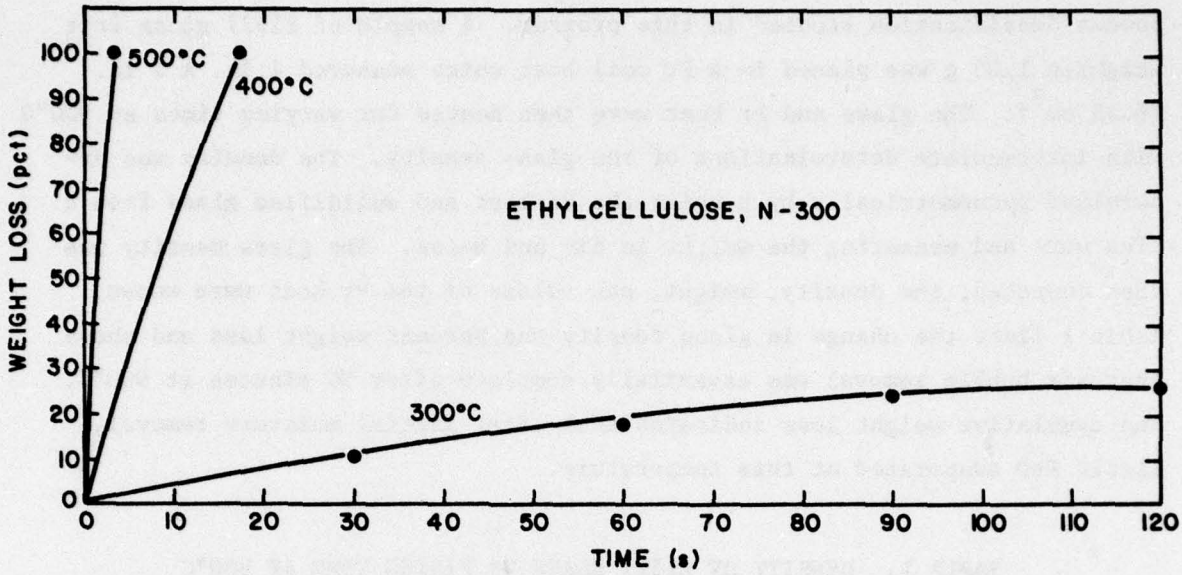

Figure 1. Polymer combustion rate.

diameter circle; this corresponds to 1.4×10^{-2} g/cm^2. If a thick-film gold ink contains 3 wt pct polymer, corresponding to approximately 30 wt pct vehicle, the polymer would cover 250 in^2. (1613 cm^2) per troy ounce (31.1 g). Then the polymer weight per unit area is 6×10^{-4} g/cm^2 and is 10 vol pct of the conductor film thickness. On the basis of this example it appears high improbable that the polymer combustion curve would seriously overlap with a metal sintering curve. If the glass sinters at a lower temperature than the metal constituents, exit paths for the polymer combustion products still exist in the unsintered metal network which typically comprises 90 vol pct of the film. Consequently, organic polymer burnout is expected to be complete before the major sintering reactions occur.

B. MK-2 Au DENSIFICATION IN THE PRESENCE OF E1527 GLASS

Since metal powder is densifying simultaneously with the glass frit, a limiting factor is the rate of air bubble escape from the molten glass. This escape rate is, in turn, controlled by the glass viscosity, which decreases exponentially with increasing temperature. To determine the escape rate, an initial experiment was conducted at 900°C, the temperature of fastest metal

powder densification studied in this program. A sample of E1527 glass frit weighing 1.05 g was placed in a Pt foil boat which measured 1 in. x 1 in. (6.45 cm^2). The glass and Pt boat were then heated for varying times at 900°C with intermediate determinations of the glass density. The density was determined pycnometrically by hanging the Pt boat and solidified glass from a fine wire and measuring the weight in air and water. The glass density was then computed; the density, weight, and volume of the Pt boat were known. Table 1 lists the change in glass density and percent weight loss and shows that air bubble removal was essentially complete after 90 minutes at 900°C. The cumulative weight loss indicates that after initial moisture removal, little PbO evaporated at this temperature.

TABLE 1. DENSITY OF E1527 GLASS VS FIRING TIME AT 900°C

Time, min	10	20	30	90	120
Density, g/cm^3	3.48	3.70	3.85	4.02	4.07
% of Theoretical Density	86	91	95	99	100
Cumulative Weight Loss, %	0.48	0.50	0.51	0.55	0.65

If we assume a uniform coating of glass in the Pt boat, ignoring the slight buildup at corners and edges, the glass thickness is:

$$\text{thickness} = \frac{\text{volume}}{\text{area}} = \frac{\text{mass/density}}{\text{area}} = \frac{1.05\ g/3.48\ g/cm^3}{6.45\ cm^2} = 0.047\ cm$$

and the slowest possible bubble escape rate is:

$$\text{rate} = \frac{\text{thickness}}{\text{time}} = \frac{0.047\ cm}{90\ min} = 5.2 \times 10^{-4}\ cm/min$$

In a conventional thick film with a fired deposit of 15 μm containing 10 vol pct glass, the glass film would be 1.5 μm (1.5×10^{-4} cm) presum-

ing uniform dispersion. The time required for complete bubble escape is:

$$\text{time} = \frac{\text{distance}}{\text{rate}} = \frac{1.5 \times 10^{-4} \text{ cm}}{5.2 \times 10^{-4} \text{ cm/min}} = 0.29 \text{ min (17 s)}$$

Referring to Fig. 6 in Quarterly Report No. 2 [1], the densification of MK-2 Au is about half-completed in 17 s at 900°C. Therefore, it is not probable that air would be confined in the glass by lack of an open path in the simultaneously densifying metal powder.

To illustrate the influence of 10 to 50 vol pct glass content and temperature on metal densification, 0.5 in. (12.7 mm)-diameter powder compacts pressed at 475 lb (215 kg), and weighing 0.85 g, were heated at 500°, 700°, 800°, and 900°C for 30 and 600 s, respectively. The plots for normalized densification*, D_n, for 30 and 600 s, appearing in Figs. 2 and 3 show D_n is directly proportional to glass content for 700°C and higher temperatures. At 500°C, i.e., barely above the glass softening point, glass content does not change D_n in the first 30 s, as shown in Fig. 2, but has a negative effect on D_n for the 600-second samples shown in Fig. 3. Therefore, as a liquid, glass very definitely assists in the first or rearrangement stage of sintering. For temperatures below or slightly above the softening point, increasing glass content retards metal densification.

Theoretically, when $D_n = 100$, the powder compact has completely densified; thus the values above 100 are erroneously high in Figs. 2 and 3. A review of weight loss data in Table 2 indicates fair stability with only minor weight losses for most compacts, with the exception of the higher glass content samples fired at 900°C. It was noted that the higher glass content samples produced glass-encased gold pellets, and that the encasing glass had wet the wire sample support. When the samples were pulled from the supporting wires, ridges were exposed where glass had formed around the wire. The ridges caused errors in compact thickness measurement, and these are probably the major cause for the D_n values which are greater than 100. It was noted that some oxides were transferred to and from the sample pellet and the wire.

* $D_n = \left(\frac{D_f - D_i}{D_t - D_i}\right) \times 100$, where D_f = final density; D_i = initial density; D_t = theoretical density.

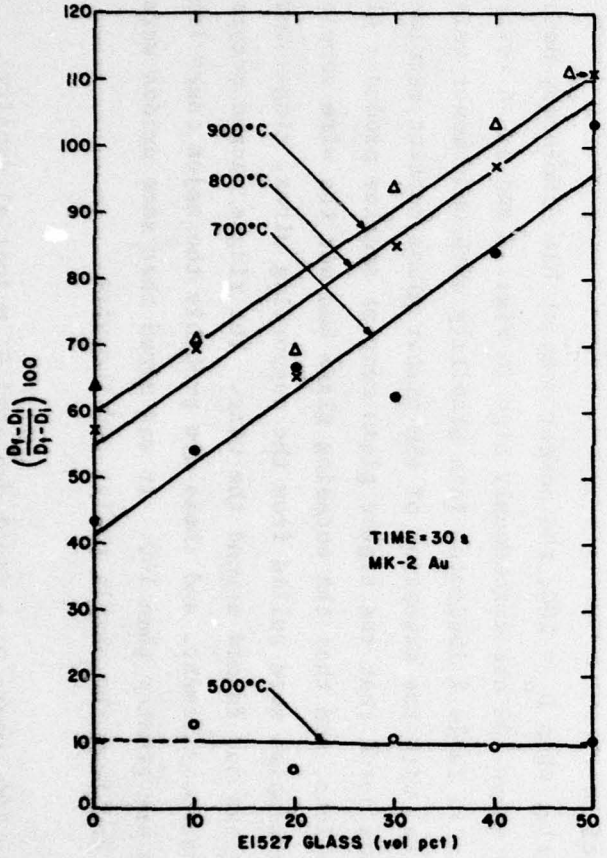

Figure 2. Normalized densification at 30 s vs temperature and glass content.

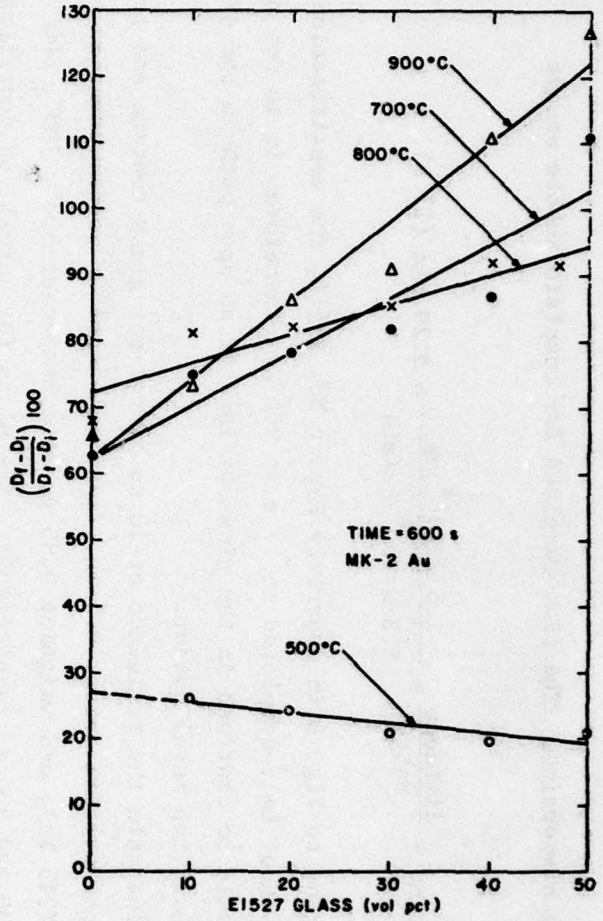

Figure 3. Normalized densification at 600 s vs temperature and glass content.

TABLE 2. PERCENT WEIGHT LOSS OF POWDER COMPACTS

Time (s)	Glass (vol pct)	Temperature (°C) 500	700	800	900
30	0	0.04	0.05	0.06	0.08
	10	0.02	0.03	0.03	0.06
	20	0.01	0.03	0.03	0.03
	30	0.01	0.03	0.02	0.01
	40	0.02	0.04	0.02	0.02
	50	0.03	0.04	0.03	0.06
600	0	0.06	0.06	0.06	0.05
	10	0.00	0.04	0.05	0.06
	20	0.02	0.03	0.04	0.06
	30	0.01	0.03	0.03	0.13
	40	0.03	0.02	0.05	0.32
	50	0.03	0.04	0.09	0.49

When D_n is compared for samples containing no glass and 10 vol pct glass, for times of 30 to 2400 s, D_n is invariably greater for the glass-bearing samples, as shown in Fig. 4 for 700°, 800°, and 900°C firings. While linear plots are used for the sake of clarity, it is recognized that the coefficient of determination, r^2, values are low, indicating a poor fit to a straight line. This effect is not unexpected since the measured time interval covers the three stages of sintering and densification rates which vary significantly in each stage. Notice, also in Fig. 4, that the glass-free gold compacts exhibit the familiar swelling problem associated with compact sintering, despite the use of the lower compaction force of 475 lb (215 kg).

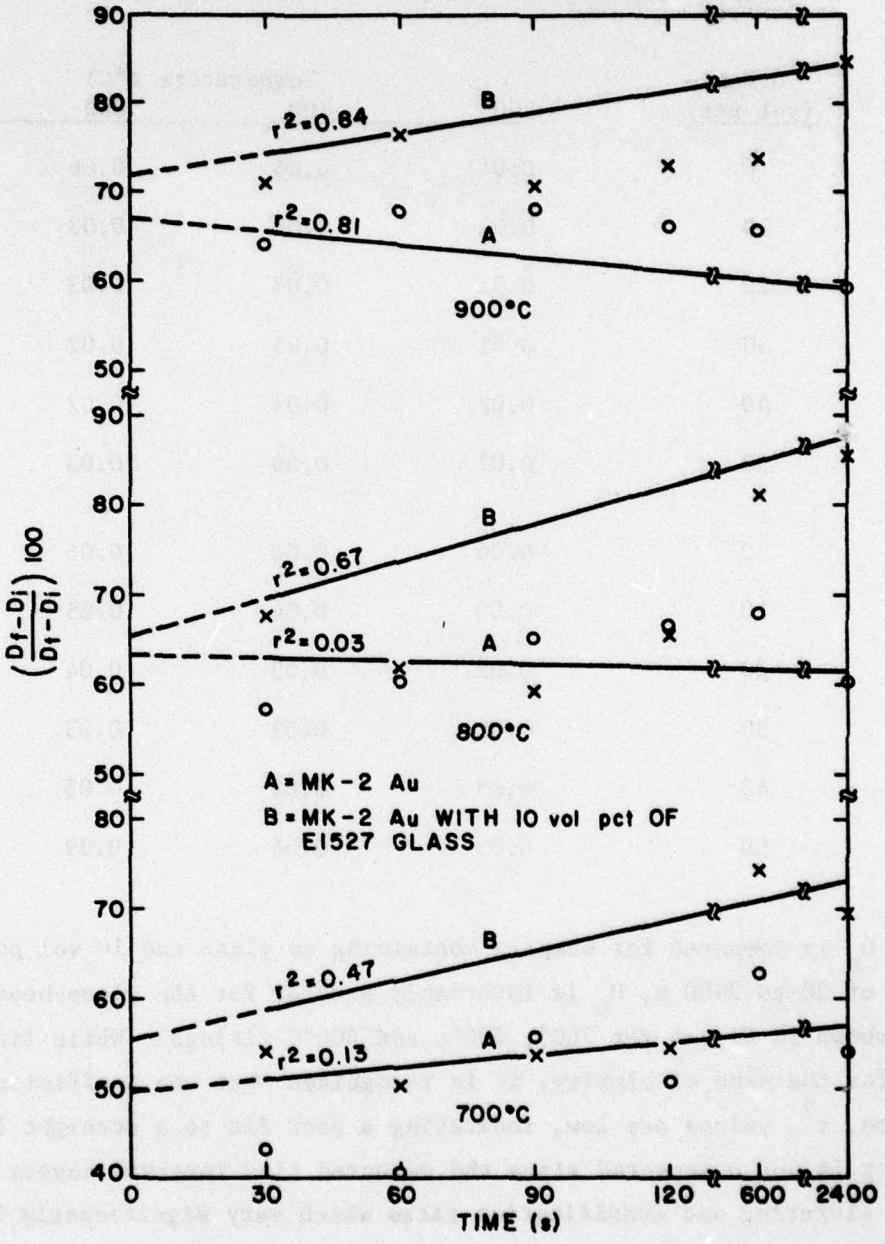

Figure 4. Normalized densification at 10 vol pct glass vs temperature and time.

C. ACTIVATION ENERGIES FOR THE SINTERING OF GOLD IN THE PRESENCE AND ABSENCE OF GLASS

The powder compact diametral changes as a function of time, $t^{0.31}$, (t = 40, 60, 90, 120, 600, and 2400 s) and temperature (700°, 800°, and 900°C) are plotted in Figs. 5 and 6 and tabulated in Tables 3 and 4 for the glass-free and glass-bearing (10 vol pct) samples, respectively. In addition, in Tables 3 and 4, the percent of theoretical density, D_t, change in actual density D_a, and normalized density, D_n, are also tabulated.

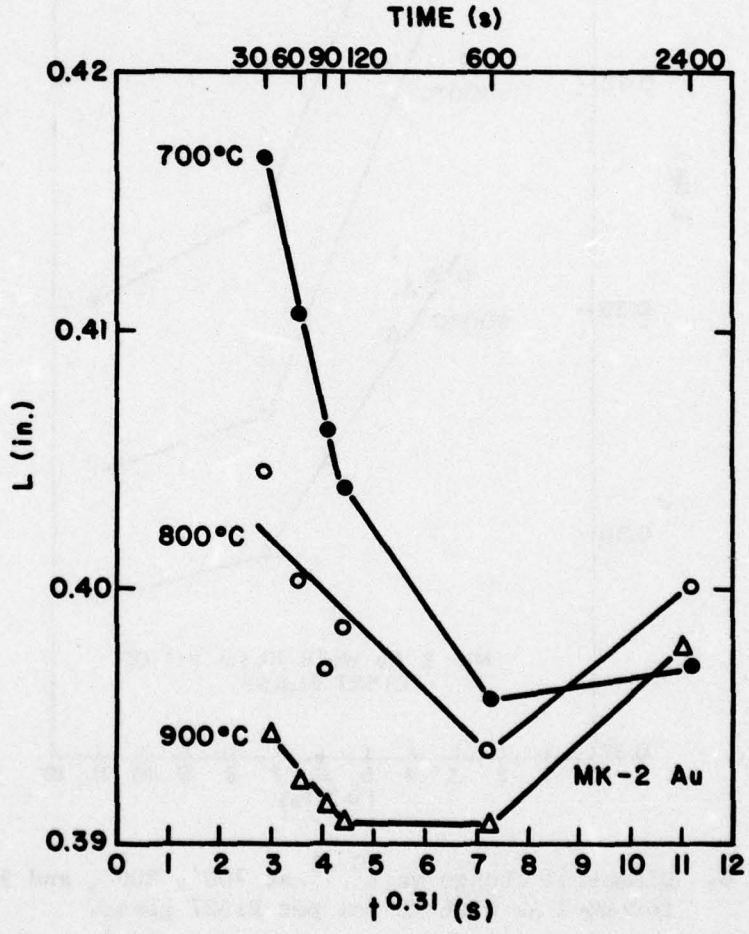

Figure 5. Diametral change vs $t^{0.31}$ at 700°C, 800°C, and 900°C for glass-free MK-2 Au.

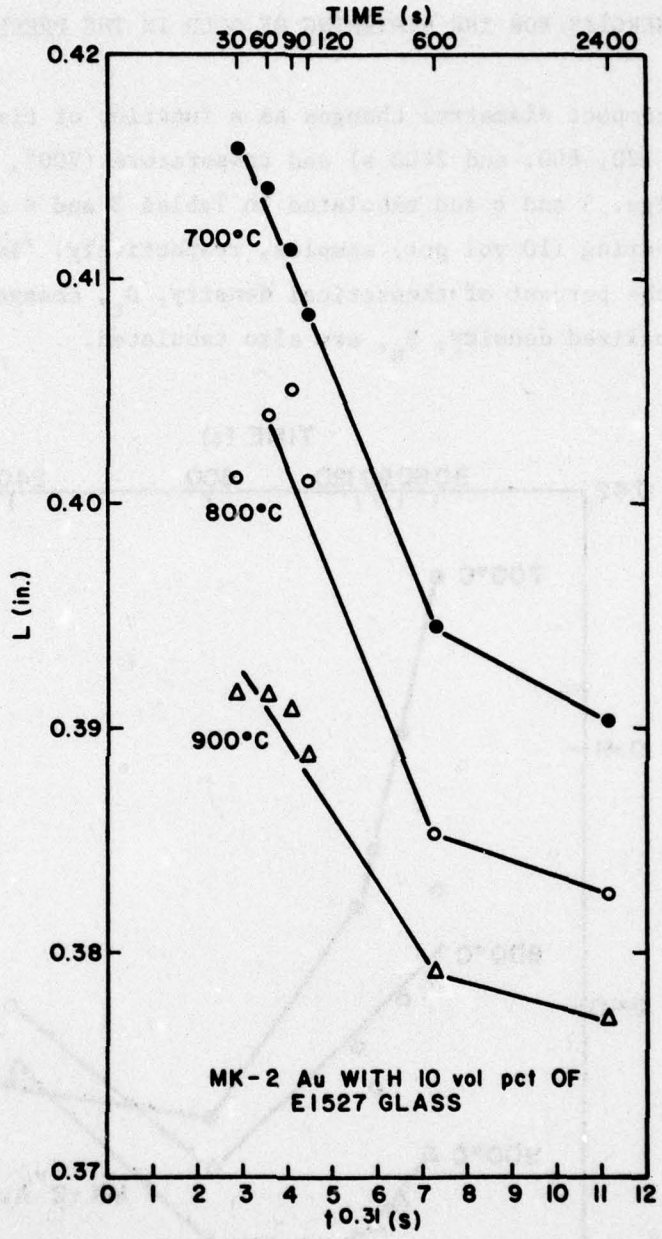

Figure 6. Diametral change vs $t^{0.31}$ at 700°, 800°, and 900°C for MK-2 Au with 10 vol pct E1527 glass.

TABLE 3. DIAMETRAL AND DENSITY CHANGES OF MK-2 Au

Temp. (°C)	Time (s)	As-Pressed Diameter L(in.)	475 lb D_t (1)	Sintered Diameter L(in.)	Sintered D_t (1)	Sintered D_n (2)	Sintered D_a (3)
700	30	0.50075	41.1	0.41607	66.6	43.3	62.2
	60	0.5007	41.4	0.40853	65.1	40.5	57.3
	90	0.50010	41.3	0.40537	74.0	55.7	79.2
	120	0.50011	41.6	0.40423	71.3	50.8	71.3
	600	0.50048	41.1	0.39576	78.0	62.7	90.0
	2400	0.50011	43.6	0.40683	74.2	54.3	70.3
800	30	0.50019	42.5	0.40448	75.6	57.7	77.8
	60	0.50020	41.9	0.40027	76.6	60.4	83.7
	90	0.50050	41.5	0.39694	79.6	65.1	91.9
	120	0.50025	42.6	0.39849	80.8	66.5	89.6
	600	0.50010	42.7	0.39367	81.6	67.9	91.3
	2400	0.50018	41.9	0.40010	76.9	60.2	83.3
900	30	0.50031	41.6	0.39421	76.4	64.2	90.1
	60	0.50046	41.6	0.39242	79.6	67.6	94.9
	90	0.50021	41.7	0.39162	76.1	68.2	95.5
	120	0.50028	41.3	0.39097	77.6	66.1	94.0
	600	0.50021	41.2	0.39088	78.0	65.6	93.6
	2400	0.50022	41.5	0.39777	84.0	59.0	83.2

1) $D_t\ (\%) = \frac{\text{observed density}}{\text{theoretical density}} \times 100$

2) $D_n\ (\%) = \left(\frac{D_f - D_i}{D_t - D_i}\right) \times 100$, where D_f = final density, D_i = initial density

3) $D_a\ (\%) = (D_f - D_i)/D_i \times 100$

TABLE 4. DIAMETRAL AND DENSITY CHANGES OF MK-2 Au WITH 10 VOL PERCENT E1527 GLASS

Temp. (°C)	Time (s)	Diameter L(in.)	D_t (1)	Diameter L(in.)	D_t (1)	D_n (2)	D_a (3)
700	30	0.50088	43.7	0.41577	74.1	54.0	69.4
	60	0.50052	43.2	0.41398	71.7	50.2	65.9
	90	0.50069	43.1	0.41133	73.6	53.7	70.8
	120	0.50041	42.8	0.40833	74.0	54.6	73.1
	600	0.50068	42.7	0.39449	85.2	74.2	99.5
	2400	0.50061	42.4	0.39033	82.5	69.6	94.4
800	30	0.50081	43.7	0.40112	82.9	69.6	89.7
	60	0.50050	42.9	0.40394	78.2	61.8	82.3
	90	0.50078	42.3	0.40509	76.5	59.3	81.0
	120	0.50064	42.8	0.40095	80.5	65.9	87.9
	600	0.50069	42.2	0.38529	89.1	81.2	111.3
	2400	0.50070	42.8	0.38264	91.8	85.7	114.6
900	30	0.50053	41.4	0.39154	82.9	70.8	100.1
	60	0.50041	42.8	0.39142	86.4	76.2	102.0
	90	0.50068	41.5	0.39085	82.7	70.4	99.3
	120	0.50055	42.3	0.38876	84.3	72.7	99.3
	600	0.50037	42.1	0.37914	84.7	73.5	101.1
	2400	0.50051	41.6	0.37708	91.2	85.0	119.3

1) $D_t\ (\%) = \frac{\text{observed density}}{\text{theoretical density}} \times 100$

2) $D_n\ (\%) = \left(\frac{D_f - D_i}{D_t - D_i}\right) \times 100$, where D_f = final density, D_i = initial density

3) $D_a\ (\%) = (D_f - D_i)/D_i \times 100$

Following the work of Johnson and Cutler [2,3], the fractional shrinkage, $\Delta L/L_o$, varies according to:

$$\frac{\Delta L}{L_o} = \left(\frac{K'D_B}{T}\right)^m t^m \tag{1}$$

where K' = constant

D_B = grain boundary diffusion coefficient

T = absolute temperature

t = time.

The value of m for grain boundary diffusion controlled sintering is 0.31. Other values range from 0.25 to 0.50 depending upon which particular diffusion path is invoked. To eliminate the effect of shrinkage errors, ΔL can be replaced by $L_o - L$ in Eq. (1) and expressed as [2,3]:

$$L = (L_o - \delta L)\left[1 - \left(\frac{K'D_B}{T}\right)^m t^m\right] \tag{2}$$

where δL is a correction for thermal expansion.

Because the powder compacts were heated for given periods of time, cooled, and then measured in a manner similar to Cole [4], the correction for thermal expansion is no longer required and (2) can be written:

$$L = L' - L'\left(\frac{K'D_B}{T}\right)^m t^m \tag{3}$$

$$\text{where } L' = L_o - \delta L. \tag{4}$$

Similarly, errors in time measurement are reduced, since sintering time was begun only when the compact reached the sintering temperature of interest.

Equation (3) fits the straight line form, if L is plotted vs t^m. Log $K'D_B$ can then be extracted from the slope and plotted against 1/T to determine

2. D. L. Johnson and I. B. Cutler, "Diffusion Sintering: I, Initial Stage Sintering Models and Their Application to Shrinkage of Powder Compacts," J. Amer. Cer. Soc. 46, 541 (1963).
3. D. L. Johnson and I. B. Cutler, "Diffusion Sintering: Initial Sintering Kinetics of Alumina," J. Amer. Cer. Soc. 46, 545 (1963).
4. S. S. Cole, "Sintering of Ag-Pd in the Presence of a Reactive Glass," J. Amer. Cer. Soc. 55, 296 (1972).

the activation energy for each stage of sintering. We have arbitrarily set t = 30 s as the limit to the first stage of sintering and found the activation energy to be 10.4 to 12.4 kcal/mole as shown for various values of t^m in Table 5. These values are sufficiently close to 15 kcal/mole recently reported by Nordstrum [5] to suggest that the first stage of sintering is completed in about 30 s. With regard to the second stage, scatter in the 800°C data and the onset of compact swelling at higher temperature and longer time caused us to examine both 120 and 600 s limits. The most credible activation energy value for the glass-free compact sintering is 42.5 kcal/mole where $t^{0.31}$ is used. This value is in very good agreement with the 41.7 kcal/mole reported by Makin, et al. [6]. The third stage activation energies are not reported for the glass-free compacts because of the presence of swelling in this time regime.

Second stage sintering in the presence of glass produces the best fit if values of t for 30 to 600 s are used as shown in Table 5. Values for activation energy range from 13.2 to 16.8 kcal/mole. The third stage values for activation energy appear to be higher in the glass-bearing samples, but these values must be suspect because of the general propensity for swelling at extended sintering time.

If $K'D_B/T$ is replaced by K_o in Eq. (3), the respective slopes of the glass-free and glass-bearing compacts can be compared at constant temperature. Solution-precipitation controlled sintering can be assumed to be operating if K_o-(glass-free) < K_o-(glass-bearing) in Stage II. From Table 6 it can be seen that a progressive decrease in the ratio K_o-(glass-free)/K_o-(glass-bearing) occurs with increasing temperature. It thus appears that the contribution to sintering by the solution-precipitation process becomes more effective at high temperatures, while grain-boundary diffusion prevails at lower temperatures.

5. T. V. Nordstrum, "Sintering Kinetics of Reactively Bonded Thick-Film Gold," presented at Fall Meeting, Amer. Cer. Soc. Electronics Div., Sept. 18-21, 1977, Montreal, Quebec, Canada.
6. S. M. Makin, et al., "Self-Diffusion in Gold," Proc. Phys. Soc. 70B, 545 (1957).

TABLE 5. SUMMARY OF ACTIVATION ENERGIES

Glass (vol pct)	Stage	Time (s)	$t^{0.31}$ r^{2*} 700°C	800°C	900°C	Q (Kcal/mole)	r^{2*}
0	I	0-30	1.0	1.0	1.0	10.4	0.999
	II	30-120	0.952	0.813	0.989	42.5	0.979
	II	30-600	0.884	0.783	0.543	64.7	0.942
	III	600-2400	-	-	-	-	-
10	I	0-30	1.0	1.0	1.0	11.3	0.993
	II	30-120	0.941	0.033	0.682	38.3	0.262
	II	30-600	0.993	0.815	0.957	13.2	0.896
	III	600-2400	1.0	1.0	1.0	22.3	0.991
			$t^{0.33}$				
0	I	0-30	1.0	1.0	1.0	12.4	0.999
	II	30-120	0.950	0.812	0.986	53.3	0.980
	II	30-600	0.879	0.777	0.534	81.1	0.942
	III	600-2400	-	-	-	-	-
10	I	0-30	1.0	1.0	1.0	13.4	0.993
	II	30-120	0.942	0.027	0.685	47.9	0.242
	II	30-600	0.993	0.823	0.960	16.8	0.893
	III	600-2400	1.0	1.0	1.0	27.7	0.985
			$t^{0.25}$				
0	I	0-30	1.0	1.0	1.0	12.4	0.999
	II	30-120	0.956	0.821	0.988	52.7	0.978
	II	30-600	0.899	0.800	0.568	79.7	0.943
	III	600-2400	-	-	-	-	-

*r^2 = coefficient of determination

TABLE 5. SUMMARIES OF ACTIVATION ENERGIES (Continued)

Glass (vol pct)	Stage	Time (s)	$t^{0.25}$ r^{2*} 00°C	$t^{0.25}$ r^{2*} 800°C	$t^{0.25}$ r^{2*} 900°C	Q (Kcal/mole)	r^{2*}
10	I	0-30	1.0	1.0	1.0	13.4	0.993
	II	30-120	0.936	0.031	0.673	47.5	0.261
	II	30-600	0.991	0.798	0.948	16.8	0.912
	III	600-2400	1.0	1.0	1.0	27.6	0.986
			$t^{0.5}$				
0	I	0-30	1.0	1.0	1.0	12.4	0.999
	II	30-120	0.935	0.791	0.977	53.8	0.982
	II	30-600	0.836	0.731	0.471	83.4	0.941
	III	600-2400	-	-	-	-	-
10	I	0-30	1.0	1.0	1.0	13.4	0.993
	II	30-120	0.956	0.018	0.713	48.3	0.200
	II	30-600	0.992	0.864	0.978	16.6	0.853
	III	600-2400	1.0	1.0	1.0	27.9	0.985

*r^2 = coefficient of determination

TABLE 6. SUMMARY OF SINTERING KINETICS OF POWDER COMPACTS

Temp. (°C)	Glass (vol pct)	$L'(K_o)^{0.31}$	L (in.)	$K_o \times 10^8$	$\frac{K_o \text{ (glass-free)}}{K_o \text{ (glass-bearing)}}$
700	0*	0.00784	0.43771	232.03	4.04
	10**	0.00501	0.43095	57.43	
800	0*	0.00442	0.41649	42.96	1.12
	10**	0.00429	0.41829	38.48	
900	0*	0.00210	0.40011	4.41	0.30
	10**	0.00306	0.40187	14.62	
700	0**	0.00410	0.42415	31.72	0.55
	10**	0.00501	0.43095	57.43	
800	0**	0.00210	0.40809	4.18	0.11
	10**	0.00429	0.41829	38.48	
900	0**	0.00060	0.39467	0.08	0.01
	10**	0.00306	0.40187	14.62	

*Data from t = 30, 60, 90, 120 s
**Data from t = 30, 60, 90, 120, 600 s

SECTION III

REACTIVELY BONDED CONDUCTORS

Using our reviews of Lisauskas's thesis [7] and the work of others reported in the last two reports [1,8] and the experimental findings of our earlier contracts [9,10,11], we have considered the important questions that remain unanswered concerning the mechanisms of reactive bonding. Experimental programs to elucidate two of the more critical points are reported here.

A. INTERFACE COMPOUND FORMATION STUDIES

The object of the first study was to determine important data on the kinetics of spinel formation. The method was modeled after Lisauskas's study [7], that is, oxide films were fired onto the substrates, etched to remove unreacted oxide, and the weight increase of reaction product on the substrate was studied as a function of temperature. Our experiments included CuO and CdO films to calibrate our experiments with those of Lisauskas, but study of the reaction of 3:1 and 1:3 CdO to CuO oxide mixtures with alumina was our principal reason for the experiment.

1. Procedure.

Coors ADS96F* 96 wt pct alumina substrates were marked for identification with a red EMCA** marking pencil and fired at 1000°C to react the pencil marks. The substrates were then washed in ethanol, rinsed in distilled water with

---

7. R. J. Lisauskas, "Characterization of the Reaction between Thick-Film Reactive-Bonded Gold Pastes and Alumina Substrates," Master's Thesis, Massachusetts Institute of Technology, June 1976.
8. T. T. Hitch and K. R. Bube, "Basic Adhesion Mechanisms in Thick and Thin Films," Quarterly Report No. 1, NASC Contract No. N00019-77-C-0176, 30 April 1977.
9. T. T. Hitch and K. R. Bube, "Basic Adhesion Mechanisms in Thick and Thin Films," Final Report, NASC Contract No. N00019-C-74-0270, 31 January 1975.
10. T. T. Hitch and K. R. Bube, "Basic Adhesion Mechanisms in Thick and Thin Films," Final Report, NASC Contract No. N00019-75-C-0145, 30 January 1976.
11. K. R. Bube and T. T. Hitch, "Basic Adhesion Mechanisms in Thick and Thin Films," Final Report, NASC Contract No. N00019-76-C-0256, 31 January 1977.

*Coors Porcelain Co., Golden, CO.
**Electro Materials Corporation of America, Mamaroneck, NY.

ultrasonic agitation, dried at 150°C, and baked at 600°C. After cooling to room temperature, each substrate was weighed in succession to the nearest 10^{-5} g; then each substrate was reweighed two or more times until agreement between weighings was apparent.

Inks were blended from -400 mesh reagent grade CuO, CdO, and mixtures of these oxides with CV-9 vehicle purchased from Cermalloy*. The pastes were screened with a 200-mesh screen in patterns 0.73 in. x 0.73 in. on the tared substrates. The prints were then dried for 15 minutes at 150°C and fired at 600°C in a belt kiln to remove the organic phases. To react the oxide films with the substrates, firing was performed at higher temperatures in a tube furnace equipped with a system to pull the quartz boat semiautomatically into the furnace, to allow a 30-minute soak at peak temperature, and to pull the boat from the furnace. The total time in the furnace was 36 minutes. Nominal soak temperatures of 900°, 950°, 1000°, and 1025°C were used. Each soak temperature was measured with a precision calibrated thermocouple and recorder system immediately before or after the specimens were fired.

The specimens were thoroughly etched in concentrated hydrochloric acid to remove the unreacted oxides, and then were washed, dried at 150°C, refired to drive off residual moisture, and reweighed after cooling to room temperature.

2. Results.

The data points in Figs. 7, 8, and 9 are each the natural logarithm of the average weight gain (in grams) of four substrates. The higher-temperature-fired CdO substrates showed substantial weight losses, in contrast to the data of Lisauskas. Those data are shown in Fig. 10, and the process appears to be thermally activated.

It was clear from the weight gains and the appearances (see Table 7) that the mixed-oxide films had strongly reacted on the substrates. Melting of the mixed oxide films appears to have occurred at the higher temperatures, but differential thermal analysis now under way should give a clearer picture of the reaction.

Activation energies computed from the weight gains (or losses) as functions of 1/T lines in Figs. 7, 8, 9, and 10 are compared with Lisauskas's activation

*Division of Bala Electronics, West Conshohocken, PA.

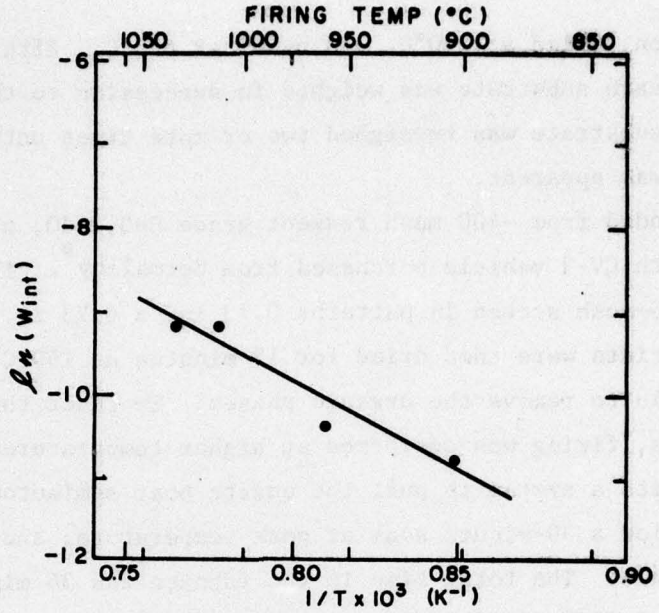

Figure 7. The reaction of CuO films with 96 wt pct alumina substrates as a function of temperature.

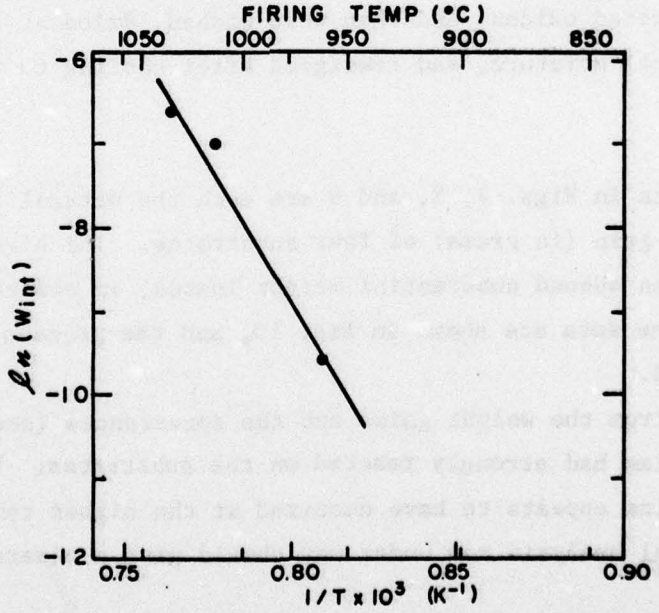

Figure 8. The reaction of 3CuO:1CdO weight mixture films with 96 wt pct alumina substrates as a function of temperature.

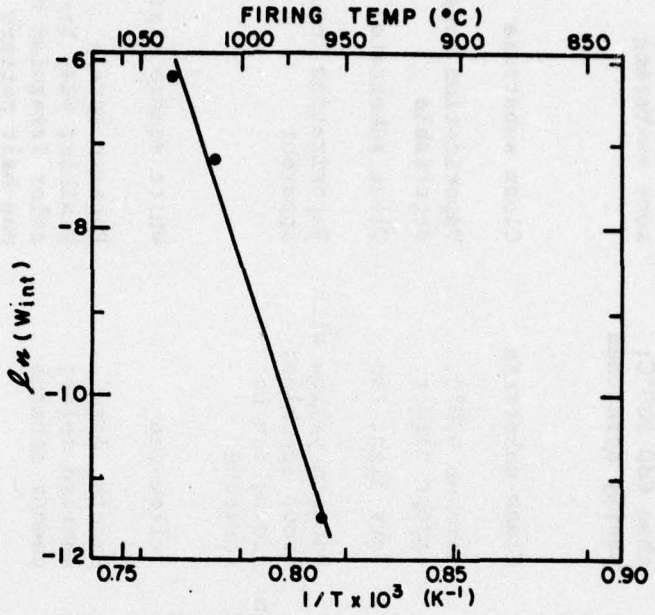

Figure 9. The reaction of 3CdO:1CuO weight mixture films with 96 wt pct alumina substrate as a function of temperature.

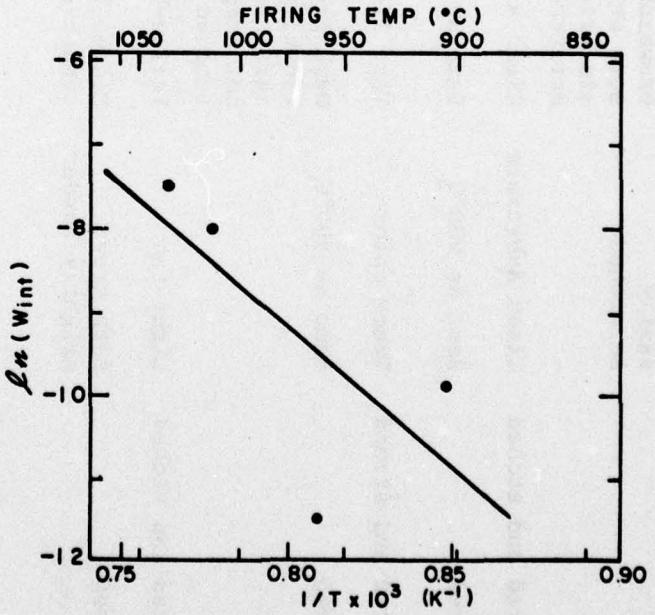

Figure 10. The reaction of CdO films with 96 wt pct alumina substrates as a function of temperature.

TABLE 7. THE CHARACTER AND APPEARANCE OF THERMALLY REACTED OXIDE FILMS ON COORS ADS96F SUBSTRATES

Firing Temp. (°C)	Condition	Oxide Paste Composition (by wt)			
		CuO	3CuO:1CdO	3CdO:1CuO	CdO
900°	Fired	Grey-black; easily scratched*	Grey-black with brownish tinge; some evidence of sintering; easily scratched	Lighter brown than CdO 900°C; easily scratched	Medium brown; some sintering
	Fired and etched	Clean substrate	Clean substrate	Clean substrate	Clean substrate
950°	Fired	Same as 900°C	Same as 900°C	Same as 900°C, except harder	Vaporization loss detectable
	Fired and etched	Trace color	Very light tan	Very light tan	Clean substrate
1000°	Fired	Same as 900°C	Dark greenish brown; can be scratched but film not completely removed	Pattern yellow with brown speckles; brown; can be scratched	Vaporization loss apparent
	Fired and etched	Light tan	Yellow-brown	Yellow-tan	White square visible
1025°	Fired	Dark grey; slightly harder	Medium brown; cannot scratch	Smooth, dark mustard color; cannot scratch	Pattern barely visible; weak brownish color irregular over one-half pattern area
	Fired and etched	Tan	Brown-yellow	Yellow-brown	White square visible

*Scratching was done with the corner of a polystyrene drafting triangle.

energies in Table 8. The CdO values are in fair agreement, except that one is a weight gain and the other a weight loss. The two CuO values are substantially different, but there are several differences between the experimental techniques which could have influenced the values.

TABLE 8. THERMAL ACTIVATION COEFFICIENTS FOR WEIGHT CHANGES DUE TO OXIDE FILM REACTIONS WITH 96 WT PCT ALUMINA SUBSTRATES

Composition (by wt)	This Study Q (Kcal/mole)	r^2 of Plotted Line	Lisauakas's Thesis[7] Q (Kcal/mole)	r^2 of Plotted Line
CuO	42 wt gain	92	87	99
3CuO:1CdO	137 wt gain	97	no data	-
1CuO:3CdO	241 wt gain	99	no data	-
CdO	68 wt loss	48	62 wt gain	99

These differences include the etchants; we used HCl, and Lisauskas used HNO_3; our greater high temperature soak times; and differences in equipment.

We caution anyone attempting experiments to react CdO with alumina at high temperatures to beware of cadmium vapors which are extremely toxic. We used 4-ft^3/h flow rate of dry air through the furnace and exhausted the furnace atmosphere into a fume hood duct. We believe this is a fairly safe approach to the experiment. A heavy condensation of cadmium-bearing solids was found to have accumulated in the exhaust end of the furnace tube. Chemical analysis is being performed to determined what other species besides cadmium were removed from the substrates to cause the weight losses.

An experiment is now required to measure weight gains at constant temperatures as a function of time at temperature. If the increases in weight are proportional to the square root of the soak time at peak temperature, this will help verify Lisauskas's model of solid-state diffusion through existent spinel as the rate-limiting step in the formation of new spinel [7,12].

12. W. D. Kingery, *Introduction to Ceramics* (John Wiley & Sons, Inc., New York, 1960) p. 335.

B. BINDER LAYER/OVERLAY EXPERIMENTS

The second series of experiments completed this quarter address the interfacial species on which adhesion depends in reactively bonded conductors. Specimens were prepared by firing layers of copper oxide, cadmium oxide, and mixtures of CdO and CuO at various temperatures onto ADS96F substrates and etching them in hydrochloric acid as described in Section III.A.1.

An overlay gold ink made from Metz 708* gold powder and CV-9 was then printed in an adhesion test pattern and fired at 900°C or 1020°C in air onto the previously prepared binder layer area of the substrate. The adhesion strength samples were Scotch-tape adherence tested. Those which passed were subjected to the recently developed, and more vigorous, soldered wire peel test [8]. The solder used was Indalloy No. 9.** None of the samples were sufficiently adherent to allow soldered wire peel test strength values to be measured, however, Table 9 indicates the adhesion of the samples. Clearly, increasing the firing temperature of the overlay gold improved the adhesion except on the substrates which had been reacted with CdO or 3CdO:1CuO at the higher temperatures. With those parts, adhesion decreased with an increase of the firing temperature of the gold film. In other experiments, two wt pct CuO was added to the Metz gold powder, blended into an ink, and fired onto the reacted and etched substrate at 1025°C. Adding copper to the gold improved its adhesion. All of the parts passed Scotch-tape testing, but none of the adhesion strengths were sufficiently great to allow the use of the conductors in hybrid circuits. It was noted that where heavy layers of reacted material had remained after etching, that some melting of the gold-two wt pct CuO film with the binder layer material occurred during the 1020°C firing. This phenomenon will receive further study.

C. DISCUSSION

On the basis of the weights of reaction product formed as a function of temperature, a mixture of CdO and CuO is more likely to bring about good adhesion strength at a lower firing temperature than CdO or CuO alone. This

*Metz Metallurgical Company, South Plainfield, NJ.
**Indium Corporation of America, Utica, NY.

TABLE 9. RESULTS OF SCOTCH-TAPE ADHESION STRENGTH TESTS ON OVERLAY GOLD FILMS FIRED ONTO THERMALLY REACTED OXIDE LAYERS ON COORS ADS96F SUBSTRATE

Oxide Layer Firing Temp. (°C)	Overlay Gold Firing Temp. (°C)	CuO	3CuO:1CdO	1CuO:3CdO	CdO
900	900	Failed	Failed	Failed	Failed
	1025	Nearly passed	Nearly passed	Partially passed	Partially passed
950	900	Failed	Failed	Failed	Failed
	1025	Nearly passed	Partially passed	Nearly passed	Failed
1000	900	Failed	Failed	Failed	Partially passed
	1025	Passed	Passed	Nearly passed	Failed
1025	900	Failed	Failed	Partially passed	Nearly passed
	1025	Passed	Passed	Passed	Failed

Note: In the order of increasing adhesion strength, the classifications are: failed, partially passed, nearly passed, and passed.

agrees with the data on reactively bonded gold and silver inks studied in earlier contract work. See Tables 18 and 19 in Ref. [10].

The "activation energies" found in this study are measures of the influence of temperature on the reaction rate but are not believed to be fundamental properties of the materials. Accordingly, their values may have been affected by experimental procedures, and the difference between our values and those of Lisauskas for CuO may thus be explainable.

The adhesion strength results of the gold overlay study are somewhat ambiguous. The 900°C fired overlays adhered best to high-cadmium films etched after firing at 1000 and 1025°C. When the overlay film was fired at 1025°C, adhesion was generally good (as measured by Scotch tape), but was poor on the higher-temperature fired samples containing greater amounts of CdO. As expected, CuO improved the adhesion, but at best, the strengths were marginal. Poor contact between the metal film and the binder layers is suspected to be the cause of the mediocre adhesion strengths. Additional work in this area is required.

IV. FUTURE WORK

With regard to the frit-bonded thick films, tests will be conducted to ascertain the extent and rate of gold dissolution in E1527 glass. Additional sintering runs at 800°C will be made to clarify the sintering kinetics in the presence and absence of glass. Attempts will finally be made to model glass flow in the presence of sintering gold on a ceramic substrate via electrical measurements and microstructural analysis.

Experiments to clarify the differences between the data of this study and that of Lisauskas are required for a better understanding of the reactive and mixed bonding mechanisms. It is anticipated that this new data will allow the correlation of these reaction rates and fundamental process data such as diffusion rates through gold films with the development of adhesion strengths in these materials. Experiments are under way in a number of areas. Critical experiments are being sought in particular to determine the following:

- The role of unreacted metal oxide in the spinel-to-metal interface of reactively bonding films.
- The importance of epitaxy in the formation of binder phase spinels, i.e., what is the influence of the presence of $MgAl_2O_4$ in the as-received substrate? (See Ref. 1)
- The influences of the ceramic and spinel on the role of the glassy layer in achieving adhesion to the metal phase in mixed-bonded inks.
- The causes of the decay of adhesion strength with over-firing reactively bonded and mixed-bonded films.

If these questions can be satisfactorily explained, adhesion of thick-film conductors will be well on the way to being understood.

IV. REFERENCES

1. K. R. Bube and T. T. Hitch, "Basic Adhesion Mechanisms in Thick and Thin Films," Quarterly Report No. 2, NASC Contract No. N00019-77-C-0176, July 1977.

2. D. L. Johnson and I. B. Cutler, "Diffusion Sintering: I, Initial Stage Sintering Models and Their Application to Shrinkage of Powder Compacts," J. Amer. Cer. Soc. 46, 541 (1963).

3. D. L. Johnson and I. B. Cutler, "Diffusion Sintering: Initial Sintering Kinetics of Alumina," J. Amer. Cer. Soc. 46, 545 (1963).

4. S. S. Cole, "Sintering of Ag-Pd in the Presence of a Reactive Glass," J. Amer. Cer. Soc. 55, 296 (1972).

5. T. V. Nordstrum, "Sintering Kinetics of Reactively Bonded Thick-Film Gold," presented at Fall Meeting, Amer. Cer. Soc. Electronics Div., Sept. 18-21, 1977, Montreal, Quebec, Canada.

6. S. M. Makin, et al., "Self-Diffusion in Gold," Proc. Phys. Soc. 70B, 545. (1957).

7. R. J. Lisauskas, "Characterization of the Reaction between Thick-Film Reactive-Bonded Gold Pastes and Alumina Substrates," Master's Thesis, Massachusetts Institute of Technology, June 1976.

8. T. T. Hitch and K. R. Bube, "Basic Adhesion Mechanisms in Thick and Thin Films," Quarterly Report No. 1, NASC Contract No. N00019-77-C-0176, 30 April 1977.

9. T. T. Hitch and K. R. Bube, "Basic Adhesion Mechanisms in Thick and Thin Films," Final Report, NASC Contract No. N00019-C-74-0270, 31 January 1975.

10. T. T. Hitch and K. R. Bube, "Basic Adhesion Mechanisms in Thick and Thin Films," Final Report, NASC Contract No. N00019-75-C-0145, 30 January 1976.

11. K. R. Bube and T. T. Hitch, "Basic Adhesion Mechanisms in Thick and Thin Films," Final Report, NASC Contract No. N00019-76-C-0256, 31 January 1977.

12. W. D. Kingery, *Introduction to Ceramics* (John Wiley & Sons, Inc., New York, 1960), p. 335.